DYNAMIC AND CONTROLLED RATE THERMAL ANALYSIS OF HYDROZINCITE AND SMITHSONITE

Veronika Vágvölgyi[1], M. Hales[2], W. Martens[2], J. Kristóf[1], Erzsébet Horváth[3] and R. L. Frost[2]*

[1]Department of Analytical Chemistry, University of Pannonia, 8201 Veszprém, PO Box 158, Hungary
[2]Inorganic Materials Research Program, School of Physical and Chemical Sciences, Queensland University of Technology
2 George Street, GPO Box 2434, Brisbane, Queensland 4001, Australia
[3]Department of Environmental Engineering and Chemical Technology, University of Pannonia, 8201 Veszprém, PO Box 158, Hungary

The understanding of the thermal stability of zinc carbonates and the relative stability of hydrous carbonates including hydrozincite and hydromagnesite is extremely important to the sequestration process for the removal of atmospheric CO_2. The hydration–carbonation or hydration-and-carbonation reaction path in the ZnO–CO_2–H_2O system at ambient temperature and atmospheric CO_2 is of environmental significance from the standpoint of carbon balance and the removal of green house gases from the atmosphere.

The dynamic thermal analysis of hydrozincite shows a 22.1% mass loss at 247°C. The controlled rate thermal analysis (CRTA) pattern of hydrozincite shows dehydration at 38°C, some dehydroxylation at 170°C and dehydroxylation and decarbonation in a long isothermal step at 190°C. The CRTA pattern of smithsonite shows a long isothermal decomposition with loss of CO_2 at 226°C. CRTA technology offers better resolution and a more detailed interpretation of the decomposition processes of zinc carbonate minerals via approaching equilibrium conditions of decomposition through the elimination of the slow transfer of heat to the sample as a controlling parameter on the process of decomposition. The CRTA technology offers a mechanism for the study of the thermal decomposition and relative stability of minerals such as hydrozincite and smithsonite.

Keywords: CRTA, hydrozincite, smithsonite, thermal analysis, thermogravimetry

Introduction

The understanding of the thermal stability of zinc carbonates and the relative stability of hydrous carbonates including hydrozincite and smithsonite is extremely important to the sequestration process for the removal of atmospheric CO_2. The hydration-carbonation or hydration-and-carbonation reaction path in the ZnO–CO_2–H_2O system at ambient temperature and atmospheric CO_2 is of environmental significance from the standpoint of carbon balance and the removal of green house gases from the atmosphere.

Smithsonite is naturally occurring zinc carbonate [1]. It is hexagonal with point group 3 bar 2/m. Carbonates with intermediate sized divalent cations normally crystallise in the calcite structure [2]. Those with larger cations have an aragonite type structure. Hydrozincite $Zn_5(CO_3)_2(OH)_6$, a mineral formed in the oxidised zones of zinc deposits, is often found as masses or crusts and is often not readily observed and may be confused with other minerals such as calcite [1]. The mineral is often associated with other secondary minerals such as smithsonite, hemimorphite, aurichalcite [1]. Hydrozincite is not commonly found as a crystalline material. Some lathe-like

or bladed crystals may be uncommonly found. The mineral is flattened on and elongated on [3] with pointed terminations up to 6 mm in length. The mineral is monoclinic with point group 2/m [4–6]. Some considerations of the stacking in the crystals have been made [5].

Of the secondary minerals of zinc only two minerals are known namely smithsonite and hydrozincite. The formation of these minerals is controlled by the partial pressure of CO_2 [7, 8]. According to the equation for the formation of hydrozincite $5ZnO(s)+2CO_2(g) \leftrightarrow Zn_5(CO_3)_2(OH)_6(s)$ with $\log K$=10.32 [7]. Thus ZnO is unstable with respect to hydrozincite at partial pressures above $10^{-5.16}$. If the partial pressure of CO_2 increases above $10^{-1.41}$ smithsonite formation is favoured according to the reaction $Zn_5(CO_3)_2(OH)_6(s)+3CO_2(g) \leftrightarrow 5ZnCO_3(s)+3H_2O(g)$. These results provide implications for the relative stability of hydrozincite and smithsonite. Thus zincite (ZnO) is a rare mineral and smithsonite is only stable at elevated CO_2 partial pressures. The partial pressure range for the stability of hydrozincite according to Williams is limited and no doubt this accounts for the rarity of the mineral in nature [8]. The mineral can be readily synthesised in the laboratory and is often

found in corrosion products of zinc [3, 9, 10]. In the presence of tenerite (CuO) the formation of malachite and/or azurite is favoured at the expense of hydrozincite [8]. Often the assemblage malachite-hydrozincite-hydrocerrusite is the stable system at 1 atmosphere CO_2 pressure. Whether these types of minerals (ZnO and CuO) can be used for the sequestration of CO_2 from the atmosphere remains to be proven. Raman spectroscopy has proven very useful for the study of minerals [11–13]. Indeed Raman spectroscopy has proven most useful for the study of diagenetically related minerals such as carbonates and hydroxycarbonate [14–18]. Some previous studies have been undertaken by the authors using Raman spectroscopy to study complex secondary minerals formed by crystallisation from concentrated sulphate solutions [12–21]. Further hot stage Raman spectroscopy is most useful for the study of the thermal decomposition of minerals [22–27]. Thermal analysis has proven most useful for the analysis of the thermal decomposition of minerals [28–40]. The aim of this paper is to present the thermal analysis of synthetic smithsonite and hydrozincite.
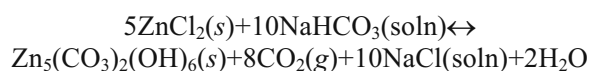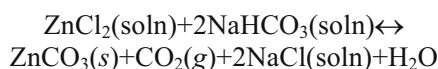
Experimental

Minerals

Synthesis of hydrozincite

Three different synthesis techniques were trialled for the synthesis of hydrozincite. The first involved weighing out equimolar amounts of the zinc(II) salt and the bi-carbonate salt, dissolving in a minimum volume of deionised water. The two zinc salts used in the experiment were zinc chloride ($ZnCl_2$) and zinc nitrate ($Zn(NO_3)_2$). Sodium hydrogen carbonate ($NaHCO_3$) was the source of the carbonate ion used for the experiments.

The following chemical reaction occurs with the reaction generating an atmosphere of CO_2.

$$5ZnCl_2(s)+10NaHCO_3(soln)\leftrightarrow$$
$$Zn_5(CO_3)_2(OH)_6(s)+8CO_2(g)+10NaCl(soln)+2H_2O$$

Smithsonite is formed according to the following reaction:

$$ZnCl_2(soln)+2NaHCO_3(soln)\leftrightarrow$$
$$ZnCO_3(s)+CO_2(g)+2NaCl(soln)+H_2O$$

Whether hydrozincite or smithsonite is obtained depends upon the partial pressure of CO_2.

The second experiment involved a similar process of mixing the reactants but at a controlled rate using a peristaltic pump system operating at 10 cm min^{-1}. The pH of the reaction was monitored but remained essentially constant at pH=7.2.

The following alternative reaction is envisaged for the formation of smithsonite:

$$Zn_5(CO_3)_2(OH)_6(s)+3CO_2(g)\leftrightarrow5ZnCO_3(s)+3H_2O(g)$$
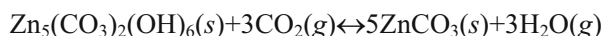
The third synthesis method involved hydro-thermally treating some of the products from the previous two methods in a hydrothermal bomb at 100°C for 48 h with adequate washing of the products after removal from the bomb. Washing was deemed to be complete when the wash water no longer gives a positive silver chloride test, indicating free chloride ions were removed. All of the samples were then washed and dried with ethanol and were placed in an oven at 80°C to dry thoroughly.

From the XRD analysis, it was found that there were some impurities of another synthetic mineral found in the samples that had both used zinc chloride and had then been hydro-thermally treated. It can be seen that hydrothermal treatment actually promotes the formation of this synthetic mineral identified as simonkolleite, a zinc chloride hydroxide hydrate mineral with the formula of $Zn_5(OH)_8Cl_2H_2O$. It is apparent that if the sample was synthesised using the $ZnCl_2$ and then hydro-thermally treated, the carbonate yield decreased significantly thereby increasing the yield of simonkolleite.

The synthesised mineral was characterised for phase specificity using XRD, and chemical composition by EDX methods

Thermal analysis

Dynamic experiment

Thermal decomposition of the samples was carried out in a Derivatograph PC type thermoanalytical equipment (Hungarian Optical Works, Budapest, Hungary) capable of recording the thermogravimetric (TG), derivative thermogravimetric (DTG) and differential thermal analysis (DTA) curves simultaneously. The sample was heated in a ceramic crucible in static air atmosphere at a rate of 5°C min^{-1}.

Controlled rate thermal analysis experiment

Thermal decomposition of the samples was carried out in a Derivatograph PC-type thermoanalytical instrument in a flowing air atmosphere (250 cm^3 min^{-1}) at a pre-set, constant decomposition rate of 0.10 mg min^{-1}. (Below this threshold value the samples were heated under dynamic conditions at a uniform rate of 1.0°C min^{-1}). The samples were heated in an open ceramic crucible at a rate of 1.0°C min^{-1} up to 300°C. With the quasi-isothermal, quasi-isobaric heating program of the instrument the furnace temperature was regulated precisely to pro-

vide a uniform rate of decomposition in the main decomposition stage.

Results and discussion

Dynamic thermal analysis of hydrozincite

The thermogravimetric and differential thermogravimetric analyses are shown in Fig. 1. In the TG curves mass loss starts at around 155 and is complete by 340°C. The main mass loss occurs at 247°C with a mass loss of 22.1%. A mass loss of 1.6% is observed between ~250 and 1000°C.
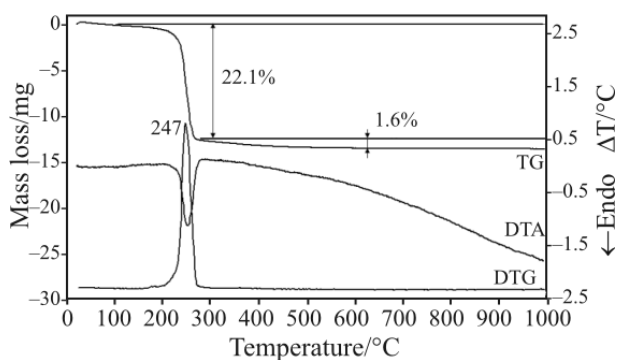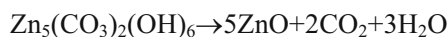

Fig. 1 Dynamic thermal analysis of hydrozincite

The theoretical mass loss may be calculated according to the equation:

$$Zn_5(CO_3)_2(OH)_6 \rightarrow 5ZnO + 2CO_2 + 3H_2O$$

This value equals 25.89%. The theoretical mass loss of CO_2 is 16.04% and for OH units is 9.85%. The dynamic thermal analysis patterns do not provide any evidence for the OH and CO_2 units being lost separately. The observed total mass loss is 22.1%. The difference is accounted for by the loss due to the formation of a second phase namely simonkolleite. The ion current curves show the temperature of the thermal decomposition as measured by gas evolution as 240°C. Other gas evolution steps are observed at 48 and 134°C. The DTA curve shown in Fig. 1 shows a strong endothermic peak at 247°C. In the DTA patterns reported by Beck [41] a large endothermic peak was found at 310°C and it was found that H_2O and CO_2 are lost simultaneously. The product of the reaction was found by XRD to be ZnO.

Controlled rate thermal analysis of hydrozincite

The thermal decomposition of hydrozincite under controlled rate conditions is shown in Fig. 2. The results of the thermal decomposition are reported in Table 1. A comparison is made with the thermal de-
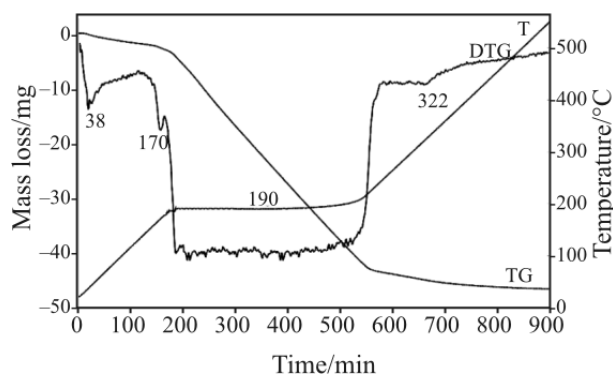


Fig. 2 Controlled rate thermal analysis of hydrozincite

Table 1 Decomposition stages of hydrozincite under dynamic conditions

Decomp. process	Temp. range/°C	Mass loss/ sample mass: 55.72 mg	
		mg	%
H_2O and CO_2 evolution	161–272	12.3	22.1
Mineral degrad.	272–605	0.9	1.6

composition of hydromagnesite under CRTA conditions in Table 1. Two decomposition steps are observed in the DTG curves at 38 and 170°C which are attributed to dehydration and dehydroxylation. Both decomposition steps are non-isothermal. There is a long isothermal decomposition step at 190°C which is attributed to the CO_2 evolution. The following reactions are envisaged:

$$Zn_5(CO_3)_2(OH)_6 \cdot xH_2O \rightarrow$$
$$Zn_5(CO_3)_2(OH)_6 + xH_2O \text{ at } 38°C$$
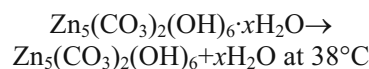
Calculations as shown in the appendix show that $x=0.31$ moles. This water is assigned to adsorbed water.

$$Zn_5(CO_3)_2(OH)_6 \rightarrow 3ZnO + 2ZnCO_3 + 3H_2O$$

$$ZnCO_3 \rightarrow ZnO + CO_2$$
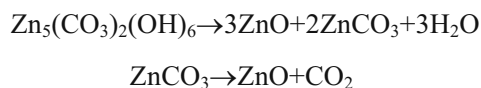
It is possible that some oxygen loss occurs at higher temperatures. The theoretical mass loss for hydrozincite based upon the formula $Zn_5(CO_3)_2(OH)_6$ is 16.03 and 9.83% for CO_2 and OH units, respectively. The mass loss for the first two steps at 38 and 170°C is 1.6%. The mass loss is 22.5% which may be compared with the total theoretical mass loss of 25.86% (16.03+9.83%).

A comparison is made between the CRTA thermal decomposition of both synthetic hydrozincite and hydromagnesite in Table 2. In the thermal decomposition of hydromagnesite significantly greater mass

Table 2 Decomposition stages of hydrozincite under CRTA conditions

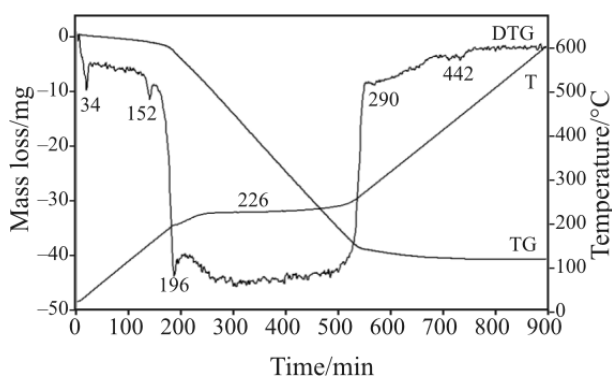| Decomposition process	Hydrozincite/sample mass: 181.29 mg			Hydromagnesite/sample mass: 99.62 mg		
	Temp. range/	Mass loss/		Temp. range/	Mass loss/	
	°C	mg	%	°C	mg	%
Dehydration	22–127	1.8	1.0	25–121	10.0	10.0
Dehydration	127–177	1.1	0.6	121–181	15.1	15.1
Dehydroxylation and Decarbonation	177–245	40.7	22.5	181–274	6.8	6.8
Decarbonation	245–367	2.0	1.1	274–394	30.0	30.1
Decarbonation	245–546	1.0	0.6	394–508	4.8	4.8

losses occur at the lower temperatures compared with that of hydrozincite. For hydrozincite the dehydroxylation and decarbonation occur simultaneously whereas for hydromagnesite in the CRTA experiment the two processes are separated. The decarbonation of hydromagnesite occurs at significantly higher temperatures.

This relative stability has implications for the sequestration of CO_2 from the atmosphere. The thermal stability of hydromagnesite is greater than hydrozincite. This suggests that MgO and $Mg(OH)_2$ would be better than ZnO and $Zn(OH)_2$ for the absorption of CO_2.

Controlled rate thermal analysis of smithsonite

The CRTA of synthetic smithsonite is reported in Fig. 3. The results of the thermal analysis are summarised in Table 3. DTG peaks are observed in similar positions to those of hydrozincite. The DTG peaks at 34, 152 and 196°C are attributed to dehydration and dehydroxylation. It is noted that thermal decomposition steps for hydrozincite occurred at 38 and 170°C. It is probable that the thermal decomposition steps of smithsonite at 34 and 152°C are due to some hydrozincite impurity.
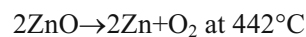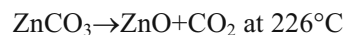
A long thermal decomposition attributed to the decarbonation of smithsonite is observed at 226°C.

Fig. 3 Controlled rate thermal analysis of smithsonite

Table 3 Decomposition stages of smithsonite under CRTA conditions

Decomposition process	Smithsonite/ sample mass: 117.08 mg		
	Temp. range/°C	Mass loss/	
		mg	%
Dehydration of adsorbed water	23–86	0.5	0.4
Hydrozincite impurity	86–163	1.0	0.9
Hydrozincite impurity ?	163–207	3.8	3.2
Decarbonation	207–274	33.8	28.9
Decarbonation	274–388	1.4	1.2
Oxygen loss	388–598	0.3	0.3

Higher temperature thermal decompositions are noted at 290 and 442°C. Based upon the formula $ZnCO_3$ the theoretical mass loss for smithsonite is 35.08%. The experimentally determined mass loss for CO_2 is 28.9%. The value is low compared with the theoretical result. Such a value is not unexpected if some hydrozincite impurity is in the synthetic smithsonite. In the DTA peak of a natural smithsonite as published by Beck [41] a large endothermic peak at 525°C is observed.
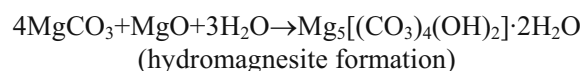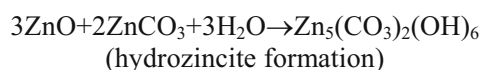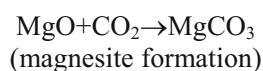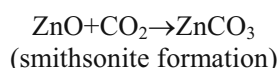
The following reactions are envisaged:

$$ZnCO_3 \cdot xH_2O \rightarrow ZnCO_3 + xH_2O \text{ at } 34°C$$

$$ZnCO_3 \rightarrow ZnO + CO_2 \text{ at } 226°C$$

$$2ZnO \rightarrow 2Zn + O_2 \text{ at } 442°C$$

It is interesting to note that many smithsonites are highly coloured due to cationic impurities. Such smithsonites may have different thermal analysis patterns to that of a pure synthetic smithsonite. The diversity of carbonate minerals has been stated to be quite remarkable [42]. The variation in chemical composition of smithsonite will affect the spectroscopic and thermal properties.

Implications for the sequestration of carbon dioxide

One proposal for the removal of green house gases from the atmosphere is to pump air into mineral beds well below the earth's surface. This process is often termed sequestration. Minerals containing zinc such as ZnO and ZnS may be suitable for the uptake of CO_2. The understanding of the thermal stability of carbonates and the relative stability of hydrous carbonates and carbonates including hydrozincite and smithsonite is extremely important to this sequestration process for the removal of atmospheric CO_2. The hydration-carbonation or hydration-and-carbonation reaction path in the $ZnO–CO_2–H_2O$ system at ambient temperature and atmospheric CO_2 is of environmental significance from the standpoint of carbon balance and the removal of green house gases from the atmosphere. Reactions are envisaged such as

$$ZnO+CO_2{\rightarrow}ZnCO_3$$
(smithsonite formation)

$$MgO+CO_2{\rightarrow}MgCO_3$$
(magnesite formation)

$$3ZnO+2ZnCO_3+3H_2O{\rightarrow}Zn_5(CO_3)_2(OH)_6$$
(hydrozincite formation)

$$4MgCO_3+MgO+3H_2O{\rightarrow}Mg_5[(CO_3)_4(OH)_2]{\cdot}2H_2O$$
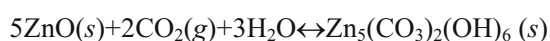(hydromagnesite formation)

These reactions are simply the reverse of the thermal decompositions of hydromagnesite, hydrozincite, magnesite and smithsonite discussed above.
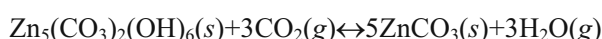
It is interesting to compare the free energy of formation of the carbonates of Zn, Mg, Ca, Sr and Ba: the values are –731.9, –1012.0, –1128.8, –1140 and –1138 kJ mol^{-1} respectively. The values suggest that $ZnCO_3$ is more easily formed compared with the other carbonates and thus would be suitable for sequestration.

Conclusions

Of the secondary minerals of zinc only two minerals are known namely smithsonite and hydrozincite and their formation of is controlled by the partial pressure of CO_2 according to the reactions

$$5ZnO(s)+2CO_2(g)+3H_2O{\leftrightarrow}Zn_5(CO_3)_2(OH)_6\ (s)$$

and

$$Zn_5(CO_3)_2(OH)_6(s)+3CO_2(g){\leftrightarrow}5ZnCO_3(s)+3H_2O(g)$$

The stability of these minerals has been determined by using thermogravimetric techniques.

The thermal decomposition of hydrozincite occurs at 247°C with an experimental mass loss of 22.1%. A further mass loss of 1.6% occurs from 300 to 1000°C. TG analysis shows that synthetic smithsonite decomposes at 226°C. A second decomposition step is observed at 152°C and is attributed to a synthetic hydrozincite impurity in the synthetic smithsonite. A total mass loss for synthetic smithsonite of 35.28% which is in excellent agreement with the theoretical mass loss of 35.2%.

CRTA technology offers better resolution and a more detailed interpretation of the decomposition processes of zinc carbonate minerals via approaching equilibrium conditions of decomposition through the elimination of the slow transfer of heat to the sample as a controlling parameter on the process of decomposition. Constant-rate decomposition processes of non-isothermal nature reveal partial collapse of the hydrozincite structure, since in this case a higher energy (higher temperature) is needed to drive out gaseous decomposition products through a decreasing space at a constant, pre-set rate. The CRTA technology offers a mechanism for the study of the thermal decomposition and relative stability of minerals such as hydrozincite and smithsonite.

Appendix

Calculation of water content for hydrozincite

Composition: $Zn_5(CO_3)_2(OH)_6{\cdot}xH_2O$
Removing water up to 127°C: 1.8 mg that is 0.100 mmol
Remaining dehydrated mineral up to 127°C: 179.49 mg that is 0.327 mmol
Molar mass of dehydrated mineral: 549.03 g mol^{-1}
Calculation of x:
1 mol dehydrated mineral – x mol H_2O
0.327 mol dehydrated mineral – 0.100 mol H_2O

$$x=0.31\ mol$$

Formula: $Zn_5(CO_3)_2(OH)_6{\cdot}0.31H_2O$

Acknowledgements

References

1 J. W. Anthony, R. A. Bideaux, K. W. Bladh and M. C. Nichols, Handbook of Mineralogy, Mineral Data Publishing, Tiscon, Arizona, USA 2003.

2 V. C. Farmer, Mineralogical Society Monograph 4: The Infrared Spectra of Minerals, 1974.

3 M. Bouchard and D. C. Smith, Asian Chem. Lett., 5 (2001) 157.

4 M. M. Harding, B. M. Kariuki, R. Cernik and G. Cressey, Acta Crystallogr., Section B: Structural Sci., B50 (1994) 673.

5 W. Zabinski, Can. Mineral., 8 (1966) 649.

6 S. Ghose, Acta Cryst., 17 (1964) 1051.

7 A. K. Alwan and P. A. Williams, Transition Metal Chem. (Dordrecht, Netherlands), 4 (1979) 128.

8 P. A. Williams, Oxide Zone Geochemistry, Ellis Horwood Ltd., Chichester, West Sussex, England 1990.

9 J. L. Jambor, Can. Mineral., 8 (1964) 92.

10 F. Zhu, D. Persson and D. Thierry, Corrosion (Houston, TX, United States), 57 (2001) 582.

11 R. L. Frost, S. J. Palmer, J. M. Bouzaid and B. J. Reddy, J. Raman Spectrosc., 38 (2007) 68.

12 R. L. Frost, D. A. Henry, M. L. Weier and W. Martens, J. Raman Spectrosc., 37 (2006) 722.

13 R. L. Frost, A. W. Musumeci, J. T. Kloprogge, M. O. Adebajo and W. N. Martens, J. Raman Spectrosc., 37 (2006) 733.

14 R. L. Frost, J. Cejka, M. Weier and W. N. Martens, J. Raman Spectrosc., 37 (2006) 879.

15 R. L. Frost, M. L. Weier, J. Cejka and J. T. Kloprogge, J. Raman Spectrosc., 37 (2006) 585.

16 R. L. Frost, J. Cejka, M. L. Weier and W. Martens, J. Raman Spectrosc., 37 (2006) 538.

17 R. L. Frost, M. L. Weier, B. J. Reddy and J. Cejka, J. Raman Spectrosc., 37 (2006) 816.

18 R. L. Frost, M. L. Weier, W. N. Martens, J. T. Kloprogge and J. Kristóf, J. Raman Spectrosc., 36 (2005) 797.

19 R. L. Frost, J. Raman Spectrosc., 37 (2006) 910.

20 R. L. Frost, R.-A. Wills, M. L. Weier and W. Martens, J. Raman Spectrosc., 36 (2005) 435.

21 R. L. Frost, A. W. Musumeci, W. N. Martens, M. O. Adebajo and J. Bouzaid, J. Raman Spectrosc., 36 (2005) 925.

22 R. L. Frost and M. L. Weier, J. Therm. Anal. Cal., 75 (2004) 277.

23 R. L. Frost, K. Erickson and M. Weier, J. Therm. Anal. Cal., 77 (2004) 851.

24 R. L. Frost, S. J. Mills and K. L. Erickson, Thermochim. Acta, 419 (2004) 109.

25 R. L. Frost, M. L. Weier and W. Martens, J. Therm. Anal. Cal., 82 (2005) 373.

26 R. L. Frost, M. L. Weier, W. Martens and S. Mills, J. Mol. Struct., 752 (2005) 178.

27 R. L. Frost, A. W. Musumeci, J. Bouzaid, M. O. Adebajo, W. N. Martens and J. T. Kloprogge, J. Solid State Chem., 178 (2005) 1940.

28 J. Bouzaid and R. L. Frost, J. Therm. Anal. Cal., 89 (2007) 133.

29 J. M. Bouzaid, R. L. Frost and W. N. Martens, J. Therm. Anal. Cal., 89 (2007) 511.

30 J. M. Bouzaid, R. L. Frost, A. W. Musumeci and W. N. Martens, J. Therm. Anal. Cal., 86 (2006) 745.

31 R. L. Frost, J. M. Bouzaid, A. W. Musumeci, J. T. Kloprogge and W. N. Martens, J. Therm. Anal. Cal., 86 (2006) 437.

32 R. L. Frost, J. Kristóf, W. N. Martens, M. L. Weier and E. Horváth, J. Therm. Anal. Cal., 83 (2006) 675.

33 R. L. Frost, J. Kristóf, M. L. Weier, W. N. Martens and E. Horváth, J. Therm. Anal. Cal., 79 (2005) 721.

34 R. L. Frost, A. W. Musumeci, M. O. Adebajo and W. Martens, J. Therm. Anal. Cal., 89 (2007) 95.

35 R. L. Frost, A. W. Musumeci, J. T. Kloprogge, M. L. Weier, M. O. Adebajo and W. Martens, J. Therm. Anal. Cal., 86 (2006) 205.

36 R. L. Frost, M. L. Weier and W. Martens, J. Therm. Anal. Cal., 82 (2005) 115.

37 R. L. Frost, R.-A. Wills, J. T. Kloprogge and W. Martens, J. Therm. Anal. Cal., 84 (2006) 489.

38 R. L. Frost, R.-A. Wills, J. T. Kloprogge and W. N. Martens, J. Therm. Anal. Cal., 83 (2006) 213.

39 A. W. Musumeci, G. G. Silva, W. N. Martens, E. R. Waclawik and R. L. Frost, J. Therm. Anal. Cal., 88 (2007) 885.

40 Y. Xi, W. Martens, H. He and R. L. Frost, J. Therm. Anal. Cal., 81 (2005) 91.

41 C. W. Beck, Am. Mineral., 35 (1950) 985.

42 L. B. Railsback, Carbonates Evaporites, 14 (1999) 1.